IOP Conference Series: Materials Science and Engineering

PAPER • OPEN ACCESS

Densification behavior of spark plasma sintered duplex stainless steel reinforced with TiN nanoparticles

To cite this article: S R Oke *et al* 2018 *IOP Conf. Ser.: Mater. Sci. Eng.* **430** 012034

IOP Conf. Series: Materials Science and Engineering **430** (2018) 012034 doi:10.1088/1757-899X/430/1/012034

Densification behavior of spark plasma sintered duplex stainless steel reinforced with TiN nanoparticles

S R Oke[1,2*], O O Ige[1,3], O E Falodun[1], M R. Mphahlele[1], PA Olubambi[1]

[1]Center for Nanoengineering and Tribocorrosion, University of Johannesburg, Johannesburg, South Africa
[2]Department of Metallurgical & Materials Engineering, Federal University of Technology Akure, Ondo State, Nigeria
[3]Department of Materials Science and Engineering, Obafemi Awolowo University, Ile-Ife, Osun State, Nigeria

*sroke99@outlook.com

Abstract. Duplex stainless steel (SAF 2205) reinforced with titanium nitride (TiN) nanoparticles ranging from 0 to 8 wt% were fabricated in vacuum via spark plasma sintering (SPS) using optimized SPS process parameter of 1150 ºC, 10 min and 100 ºC/min. The influence of TiN addition on the densification and shrinkage mechanism of the fabricated duplex stainless steel composite were evaluated. The results indicate even dispersion of the TiN nanoparticles in the steel matrix during tubular mixing. The displacement and shrinkage rates showed three densification stages relating to micro-nano particles rearrangement, plastic deformation of the particles and rapid densification of the composite. The steel composite samples displayed relatively high densities in the range of 96-99 % of the calculated theoretical density but were noted to decrease with TiN content.

1. Introduction

The development of nano-engineered materials has attracted a lot of interest from researchers in recent times. The concept requires that at least one of the components of a multiphased material be in the nano-size range (less than 100 nm) [1]. The potential of nanoparticle reinforced materials relies on their multifunctionality and their ability of achieving improved properties beyond levels obtainable with convectional materials [2]. The challenges of accomplishing homogeneous dispersion and prevention of grain growth of the nano-sized component, selection of appropriate fabrication route and understanding the role of densification in obtaining a less porous sintered product are tremendous [3-4].

This study presents an investigation into the mechanisms involved during the densification of SAF 2205 and TiN nanoparticles by SPS technique. SPS is a pressure assisted sintering technique and has been extensively used for the fabrication of different types of materials such as alloys and metals, ceramics, intermetallic and composite [5]. SPS has gained attention due to its advantages of lower sintering temperature and shorter holding time as compared with other conventional sintering processes [6]. The densification data obtained during SPS of powders can be used to have a thorough grasp of the underlying

deformation/densification mechanism during SPS [7]. A previous study by Bernard-Granger and Guizard [7] formulated a hypothesis based on creep deformation to understand the underlying mechanisms that govern densification during the SPS process. The creep model has been employed to predict the densification phenomena of metal matrix composite during the SPS but the understanding of the fundamental microscopic mechanisms of densification is still largely unexplored. In another study by Oke et al. [8] on the optimization of SPS process parameters, the authors reported that densification during SPS is achieved in three distinctive stages of powder particles rearrangement, deformation at powder contact point, and bulk deformation of the sintered material.

An attempt is therefore made in this work to study the influence of TiN nanoparticle addition on the densification mechanism of SPS consolidated duplex stainless steel samples reinforced with TiN nanoparticles.

2. Materials and method

Starting materials used in this study were commercially available SAF 2205 (C-≤0.03, Si- ≤1.0, Mn-≤2.0, P-≤0.03, S-≤0.015, Cr-22, Ni-5, Mo-3.2, N-0.18, Fe-bal wt.%) as well as TiN nanopowders (C-0.03, Si-<0.003, Ni-5, N-<21.91, Ti-77.83, Fe-<0.001 wt. %). Blending of the powders were done for 6 h at 72 rpm using a Tubular Mixer T2F. The mixed stainless steel powders with varying amount of TiN ranging from 0 to 8 % were sintered using a SPS apparatus (model HHPD-25, FCT GmbH Germany) using optimized process parameters from our previous study [8]. On the completion of SPS, the sintered samples were removed from the die and sand blasted to get rid of graphite contaminations on the surface of the samples. The sintering data was obtained and analyzed.

The morphology of the mixed powders was assessed using scanning electron microscope (FESEM, JSM-7600F, JEOL, Japan). The density of the sintered samples was determined using Archimedes technique. Six repeated tests were ensured for each sample for reliability of result. The SPS data obtained during sintering were used to analyze the densification and shrinkage mechanisms.

3. Results and discussion

3.1 Microstructure of mixed powders

The efficiency of tubular mixing of the powder particles is judged by the degree of dispersion of the reinforcing nanoparticles in the duplex matrix. Figs 1(a) and (b) present SEM morphology of admixed SAF 2205 and TiN powders. An even dispersion of the nanoparticles around the each of the SAF 2205 powder was observed. This indicates that tubular mixing is an effective method for dispersing nanoceramics in stainless steels. Fig. 1c depicts the X-ray diffraction pattern of the tubular blended powders, only peaks corresponding ferrite, austenite and TiN phase were identified. The microstructure of the unreinforced stainless steel (Figure 1d) revealed only primarily phases of ferrites (α) and austenite (γ). Energy Dispersive Spectroscopy (EDS) analysis of the composite show Cr and Mo as dominant in the α phase while Ni is dominant in the γ phase as expected. Figure 1e shows the microstructure of the duplex steel samples with 6 wt% TiN contents containing α, γ and nitride phases (evident in the XRD presented in Figure 1f) at α. γ grain boundaries. During the sintering process, the applied electrical potential causes a current flow through powder particles and is followed by sparks formation at the contact points but in the case of TiN nanoceramics and conductive DSS, a potential difference across stainless steel particles separated by the nitride phases may develop.

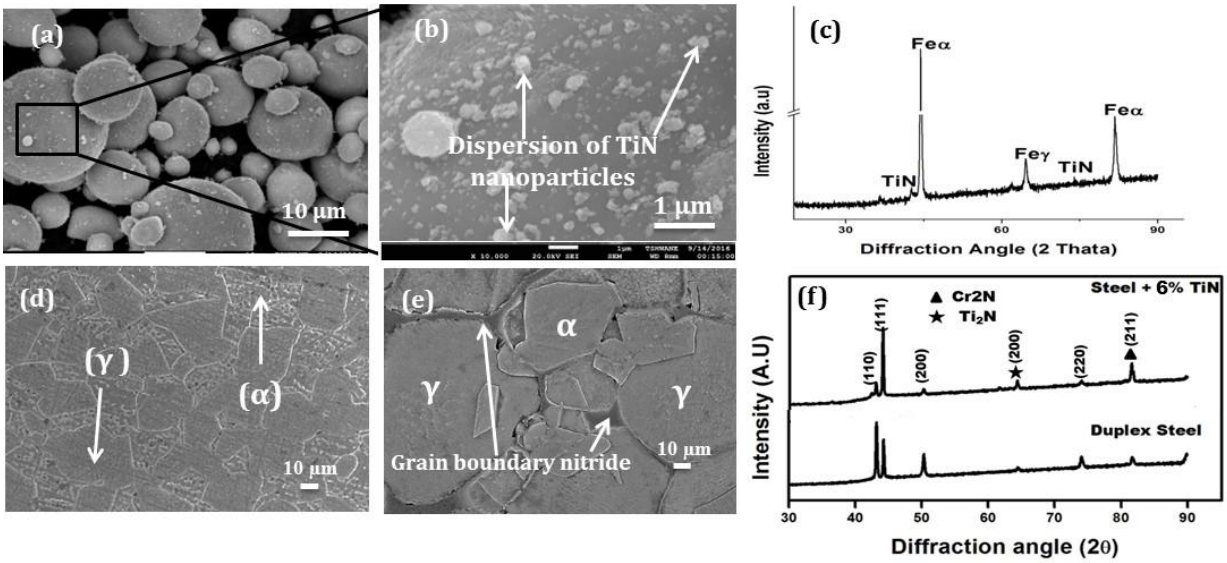

Figure 1. Micrographs showing (a) SEM of tubular mixed powders (b) High mag. Image showing dispersion of TiN nanoparticles. (c) XRD of tubular mixed powders (d) unreinforced duplex stainless steel (e) Steel composite with TiN contents (f) XRD of sintered composite showing evolution of nitride phases.

3.2. Displacement and shrinkage rates of the SAF 2205-TiN

Figures 2 and 3 present the displacement and shrinkage rates as a function of total sintering time during SPS at 1150 °C of the TiN nanoparticles reinforced stainless steel. The figures depict the densification phenomena occurring throughout the sintering process. It is noted from Figure 2 that the total sintering time increased with TiN nanoparticles. The rise in total sintering time could be due to decreased conductivity of the composite as a result of the addition of a nanoceramic phase (TiN). It is imperative to state that the SAF 2205 and TiN nanoparticles are conductive and non-conductive materials respectively, during sintering a constant pulse electric current is used to initiate a current flow through the contact point between conductive (SAF 2205) and non-conductive nanoceramics (TiN). Due to difference in thermal conductivity and potential between the SAF 2205 and TiN, an increased amount of energy is needed to raise the sintering temperature up to 1150 ^{o}C, thereby increasing the total sintering time. Similar trend in punch displacement behavior is observed for all the composite irrespective of the amount of reinforcement but the amount of total punch displacement increased with TiN content. The behavior can be attributed to increased energy devoted in consolidating the mixed powders from the initial height of powder bed to final sintered height 5 mm [9].

The shrinkage rate during SPS as a function of total sintering time for the unreinforced and 8 wt% TiN reinforced steel is shown in Figure 3. The composite displayed similar shrinkage behavior; three distinct shrinkage stages were identified. The first shrinkage stage (0 – 10 min) is characterized by initial rearrangement of the mixed powder particles, gas removal and creation of spark between SAF 2205 and TiN particles [8]. The curves revealed an increase in shrinkage rate with TiN nanoparticle additions. The enhanced shrinkage obtained for the unreinforced steel could be attributed to the low melting point of the steel as compared to the reinforced composite. Similar observation was reported by Ghasali et al., the authors argued that metal matrix with lower melting point tend to deform easily [10].

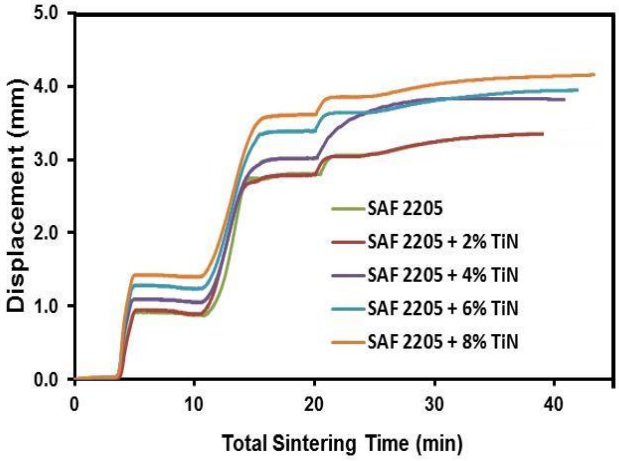

Figure 2. Variation of punch displacement with total sintering time for the SAF 2205 reinforced with TiN nanoparticles.

The second shrinkage stage which occurred between 10 – 20 min is attributed to Joule heating effect accompanied by localized plastic deformation of the particles at contact point. In this stage of SPS, powder surface activation and partial melting, formation of neck at contact points, atomic diffusion and plastic flow occurs [11]. The surface of the stainless steel and TiN nanoparticles was activated due to high pulse discharge plasma created at powder contacts. With increase in sintering temperature, sintering takes place between the powder particles due to softening effects at powder surface, thereby forming necks. At this point, joule heating becomes the dominant heating mode. Huge amount of Joule heating increases the temperature at particle surface resulting in melting, evaporation and growth of the sintering neck. Densification is enhanced at this stage and proceeds further via plastic deformation under the pressure. The third stage commenced after 20 min until the end of sintering operation, a drastic reduction in shrinkage rate was observed. This could be attributed to the decrease in temperature caused by cooling of the SPS chamber to room temperature. Densification is also completed by mass transportation at this stage [8,10.11].

3.3 Influence of TiN addition on density

The result of the relative densities of the stainless steel reinforced TiN nanoparticles is depicted in Figure 4. The steel composite samples displayed relatively high densities; the density was noted to be in the range of 96-99 % of the calculated theoretical density. This could be attributed to the positive effect of created plasma on the mobility and diffusion of atoms by vaporizing and melting of powder particle surface during SPS [12]. It was however noted that the relative density of composite decreased with an increase in TiN content of the duplex stainless steel matrix. The occurrence of the TiN reinforcing phase at boundaries tends to inhibit atomic diffusion and reduces the sintering rate during SPS (Figure 1). Owing to the complex phenomena occurring during SPS and the diffusion inhibition effect of the TiN phase, the sintered composite showed a diminishing densification with increasing TiN contents. Maja *et al.* [13] reported similar behavior with the addition of TiN to metal matrix. The authors advocated that TiN addition could decrease the contacting area between particles of the ductile metal matrix, impede their diffusion and decrease their deformation ability. These factors have an adverse influence on densification. The appropriate application of selected SPS process parameters as established in our previous study [8] resulted in near fully dense steel composite in short sintering times. In the SPS process of synthesizing SAF 2205 and TiN nanoparticles, a high temperature condition is created at the contact point of the stainless steel and TiN nanoparticles. The sparks which were generated due to applied pulsed currents causes evaporation and melting on the powder surface, thus helping in the fabrication of high-density sintered samples [14].

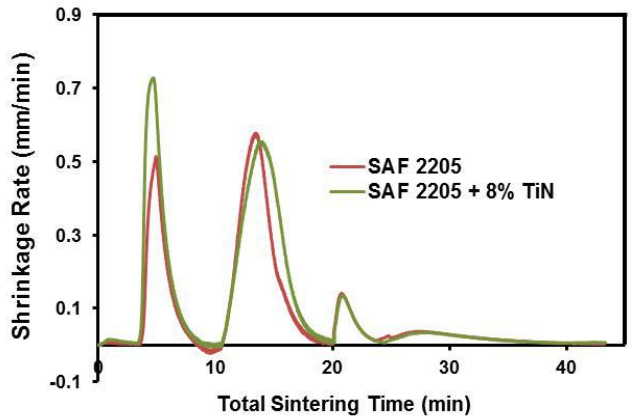

Figure 3. Variation of shrinkage rate with total sintering time of SAF 2205 reinforced with 8 wt% TiN nanoparticles.

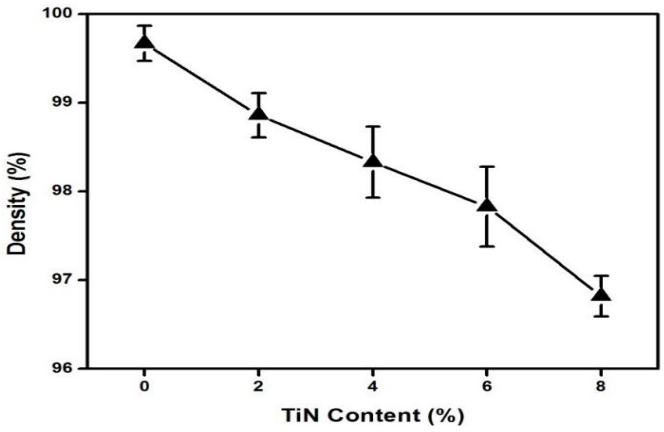

Figure 4. Variation showing decreasing trend of experimental density with the increased addition of TiN nanoparticles to duplex stainless steel.

4. Conclusions

This study fabricated duplex stainless steel reinforced with TiN nanoparticles via SPS using optimized parameters from our previous work [8]. The effects of TiN nanoparticles addition on displacement and shrinkage rate of the duplex stainless steels composite was investigated. The results are summarized as follows;

1. Similar shrinkage behavior was noted for all the composite irrespective of the amount of reinforcement but the total sintering time and punch displacement increased with increasing content of TiN nanoparticles.
2. Three densification stages characterized by powder particle rearrangement, localized plastic deformation and rapid densification by mass transport and cooling respectively were observed during SPS process.
3. TiN nano addition decreased the relative density of the stainless steel composite.

Acknowledgments

This work is supported by the National Research Foundation (NRF) of South Africa and the University of Johannesburg Global Excellence and Stature (GES).

References

[1] Ajayan P M, Schadler L S, Braun PV 2006 Nanocomposite science and technology *John Wiley & Sons*.

[2] Moya J S, Lopez-Esteban S, Pecharroman C 2007 The challenge of ceramic/metal microcomposites and nanocomposites *Prog. Mater. Sci.* **52** 1017-90.

[3] Tjong SC 2007 Novel Nanoparticle-reinforced metal matrix composites with enhanced mechanical properties *Adv. Eng. Mater*. **9** 639-52.

[4] Wang L, Zhang J, Jiang W 2013 Recent development in reactive synthesis of nanostructured bulk materials by spark plasma sintering *Int. J. Refract. Met. Hard Mater.* **39** 103-112.

[5] Oke SR, Ige OO, Falodun OE, Obadele BA, Mphahlele MR, Olubambi PA 2018 Influence of sintering process parameters on corrosion and wear behaviour of SAF 2205 reinforced with nano-sized TiN *Materials Chemistry and Physics* **206** 166-173.

[6] Diouf S, Molinari A 2012 Densification mechanisms in spark plasma sintering: Effect of particle size and pressure *Powder Technology* **221** 220 –227

[7] Bernard-Granger G, Guizard C 2007 Spark plasma sintering of a commercially available granulated zirconia powder: I. Sintering path and hypotheses about the mechanism (s) controlling densification *Acta Materialia* **55(10)** 3493-3504.

[8] Oke SR, Ige OO, Falodun OE, Obadele BA, Shongwe MB, Olubambi PA 2018 Optimization of process parameters for spark plasma sintering of nano structured SAF 2205 composite *Journal of Materials Research and Technology* **7(2)** 126-134.

[9] Cheng Y, Cui Z, Cheng L, Gong D, Wang W 2017 Effect of particle size on densification of pure magnesium during spark plasma sintering. *Advanced Powder Technology* **28(4)** 1129-1135.

[10] Ghasali E, Shirvanimoghaddam K, Pakseresht A.H, Alizadeh M, Ebadzadeh, T 2017 Evaluation of microstructure and mechanical properties of Al-TaC composites prepared by spark plasma sintering process *Journal of Alloys and Compounds* **705** 283-289.

[11] Bonifacio CS, Rufner JF, Holland TB, Van Benthem K 2012 In situ transmission electron microscopy study of dielectric breakdown of surface oxides during electric field-assisted sintering of nickel nanoparticles *Appl. Phys. Lett.* **101** 4583–4586.

[12] Song Y, Li Y, Zhou Z, Lai Y, Ye Y 2011 A multi-field coupled FEM model for one-step-forming process of spark plasma sintering considering local densification of powder material *J. Mater. Sci.* **46** 5645–5656

[13] Maja ME, Falodun OE, Obadele BA, Oke SR, Olubambi PA 2018 Nanoindentation studies on TiN nanoceramic reinforced Ti–6Al–4V matrix composite *Ceramics International* **44(4)** 4419-4425

[14] Oke SR, Ige OO, Falodun OE, Obadele BA, Mphahlele MR, Olubambi PA 2018 Dependence of wear and corrosion properties on holding time of spark plasma sintered SAF 2205 reinforced with TiN *nanoparticles InMechanical and Intelligent Manufacturing Technologies (ICMIMT) IEEE 9th International Conference* 80-84 IEEE.